



Surface Structure Characterization of *Aspergillus fumigatus* Conidia Mutated in the Melanin Synthesis Pathway and Their Human Cellular Immune Response

Jagadeesh Bayry, Audrey Beaussart, Yves Dufrêne, Meenu Sharma, Kushagra Bansal, Olaf Kniemeyer, Vishukumar Aimananda, Axel Brakhage, Srinivasa Kaveri, Kyung Kwon-Chung, et al.

► To cite this version:

Jagadeesh Bayry, Audrey Beaussart, Yves Dufrêne, Meenu Sharma, Kushagra Bansal, et al.. Surface Structure Characterization of *Aspergillus fumigatus* Conidia Mutated in the Melanin Synthesis Pathway and Their Human Cellular Immune Response: Melanin mutants of *Aspergillus fumigatus* and immune response. *Infection and Immunity*, 2014, 82 (8), pp.3141-3153. 10.1128/IAI.01726-14 . inserm-02455511

HAL Id: inserm-02455511

<https://inserm.hal.science/inserm-02455511>

Submitted on 25 Feb 2020

HAL is a multi-disciplinary open access archive for the deposit and dissemination of scientific research documents, whether they are published or not. The documents may come from teaching and research institutions in France or abroad, or from public or private research centers.

L'archive ouverte pluridisciplinaire **HAL**, est destinée au dépôt et à la diffusion de documents scientifiques de niveau recherche, publiés ou non, émanant des établissements d'enseignement et de recherche français ou étrangers, des laboratoires publics ou privés.



Distributed under a Creative Commons Attribution - NonCommercial 4.0 International License

Surface structure characterization of *Aspergillus fumigatus* conidia mutated in the melanin synthesis pathway and their human cellular immune response

Jagadeesh Bayry^{1,2}, Audrey Beaussart³, Yves F. Dufrêne³, Meenu Sharma^{1,2}, Kushagra Bansal^{1,2}, Olaf Kniemeyer^{4,5}, Vishukumar Aimaniananda⁶, Axel A. Brakhage⁴, Srini V Kaveri^{1,2}, Kyung J. Kwon-Chung⁷, Jean-Paul Latgé^{6*}, Anne Beauvais^{6*}

¹Institut National de la Santé et de la Recherche Médicale, Unité 1138, Paris, France; ²Centre de Recherche des Cordeliers, Université Pierre et Marie Curie – Paris 6, UMR S 1138, Université Paris Descartes, UMR S 1138, Paris, France; ³Université catholique de Louvain, Institute of Life Sciences, Louvain-la-Neuve, Belgium; ⁴Molecular and Applied Microbiology, Leibniz-Institute for Natural Product Research and Infection Biology (HKI), University of Jena, Germany; ⁵Integrated Research and Treatment Center, Center for Sepsis Control and Care Jena, University Hospital (CSCC), Jena, Germany; ⁶Unité des *Aspergillus*, Institut Pasteur, Paris, France; ⁷Molecular Microbiology Section, Laboratory of Clinical Infectious Diseases, NIAID, NIH, Bethesda, Maryland, USA

*Corresponding authors: Tel: (33)-145688225, Fax: (33)-1406133419, anne.beauvais@pasteur.fr; jean-paul.latge@pasteur.fr

Running title: Melanin mutants of *Aspergillus fumigatus* and immune response

Key words: *Aspergillus fumigatus*, melanin, dendritic cells, T cells, cytokines, human, conidial surface, cell wall, rodlet, hydrophobin.

24 **Abstract**

25 In *Aspergillus fumigatus*, the conidial surface contains dihydroxynaphthalene (DHN)-melanin.
26 Six-clustered gene products have been identified that mediate sequential catalysis of DHN-
27 melanin biosynthesis. Melanin thus produced is known to be a virulence factor, protecting the
28 fungus from the host defense mechanisms. In the present study, individual deletion of the genes
29 involved in the initial three steps of melanin biosynthesis resulted in an altered conidial surface
30 with masked surface rodlet layer, leaky cell wall allowing the deposition of proteins on the cell
31 surface and exposing the, otherwise masked, cell wall polysaccharides at the surface. Melanin as
32 such was immunologically inert; however, deletion mutant conidia with modified surfaces could
33 activate human dendritic cells and the subsequent cytokine production in contrast to the wild-type
34 conidia. Cell surface defects were rectified in the conidia mutated in downstream melanin
35 biosynthetic pathway and maximum immune inertness was observed upon synthesis of
36 vermelone onwards. These observations suggest that though melanin as such is an
37 immunologically inert material, it confers virulence by facilitating proper formation of the *A.*
38 *fumigatus* conidial surface.

39

40 **Introduction**

41 Melanin is a pigment that exists from humans to plants and has several functions including
42 resistance against environmental stress such as UV light and oxidizing agents (1, 2). In air-borne
43 fungal spores, melanin helps in invasion of the host (3, 4) and contributes to the virulence of
44 fungal pathogens (5, 6). Fungi produce different types of melanin: dihydroxynaphthalene (DHN)
45 melanin, pyomelanin and DOPA-melanin. *Aspergillus fumigatus* produces the pigment DHN-
46 melanin, responsible for the characteristic gray-green color of conidia. *A. fumigatus* is also able to
47 produce a brownish pigment, pyomelanin, as an alternative melanin (7). Pyomelanin is produced

48 via degradation of L-tyrosine with homogentisic acid (HGA) as the main intermediate. On the
49 other hand, *Cryptococcus neoformans* and *Paracoccidioides brasiliensis* synthesize DOPA-
50 melanin (8). Production of melanin has been associated with the survival of the fungal species in
51 the host (8, 9). DHN-melanin is hydrophobic and negatively charged, which modulates the
52 binding capacity of conidia to host fibronectin and laminin present in the lungs (10). DHN-
53 melanin is also essential for the proper assembly of cell wall layers in *A. fumigatus*. Pyomelanin
54 was shown to protect the fungus from host defense mechanism, i.e., reactive oxygen
55 intermediates, and hence considered to be protecting the fungus against immune effector cells
56 during infection (11). DOPA-melanin contributes to host death, fungal burden and dissemination
57 (8).

58
59 Genes responsible for the synthesis of DHN-melanin in *A. fumigatus* belong to a 19-kb cluster
60 located on chromosome 2. Six genes have been identified in this cluster and their functions were
61 elucidated (Fig. 1) (4-6, 12-14). The *PKSP* (*ALB1*; AFUA_2G17600) is the first gene of the
62 pathway and codes for a polyketide synthase, which is responsible for catalyzing the synthesis of
63 the heptaketide naphthopyrone from acetyl-CoA and malonyl-CoA. The heptaketide is then
64 shortened by hydrolysis, reduction and dehydration by Ayl1p (AFUA_2G17550, Arp2p
65 (AFUA_2G17560) and Arp1p (AFUA_2G17580) respectively. The generated product 1,3,6,8-
66 tetrahydroxynaphthalene (THN) is reduced again by Arp2p and the resulting vermellone is
67 oxidized by the copper oxidase Ayl1p (AFUA_2G17540) to form the 1,8 DHN melanin, which is
68 polymerized by the laccase Ayl2p (AFUA_2G17530) (12, 15).

69
70 The role of the conidial melanin in the *A. fumigatus* virulence has been studied by using either
71 melanin ghosts or the pigment-less mutant wherein *PKSP* gene, which encodes protein involved

72 in the first step of melanin biosynthesis, has been deleted (4, 9, 16-19). These reports
73 demonstrated that melanin protects the conidia against reactive oxygen species (ROS), masks the
74 recognition of various *A. fumigatus* pattern-associated molecular patterns (PAMPs), inhibits
75 macrophage apoptosis and phagolysosome fusion and attenuates the host immune response. All
76 these functions of melanin contribute to increased survival of conidia in the macrophages and to
77 promote the dissemination of *A. fumigatus* within the host.

78

79 However, the importance of melanin in the organization of the *A. fumigatus* conidial cell wall,
80 structural organization of the conidial surface due to the lack of melanin or in the presence of
81 melanin intermediates and effect of melanin intermediate biosynthetic gene deletion on the
82 activation of host immune cells are still unknown. In this study, by using melanin mutants that
83 are deleted in each of the genes of the melanin synthesis pathway, we analyzed the surface
84 structure of conidia by biochemical and biophysical methods and explored the immune-
85 modulatory role of these conidia on human dendritic cells (DCs), the professional antigen
86 presenting cells (APC) that act as sentinels of the immune system. We demonstrate for the first
87 time that until the scytalone precursor was synthesized by Arp2p, the first three melanin
88 biosynthetic gene deletion mutants ($\Delta pksP$, $\Delta ayg1$ and $\Delta arp2$) induce the maturation of DCs and
89 cytokine production. Upon vermeline biosynthesis after dehydration of the scytalone by Arp1p
90 and reduction by Arp2, the subsequent mutants ($\Delta abr1$ and $\Delta abr2$) behaved like wild-type (WT)
91 conidia, losing their capacity to prime the maturation of DCs and cytokine production. The $\Delta arp1$
92 conidia having scytalone but not vermeline on their surface were able to induce only a weak
93 maturation of DCs. Further, we found that activation of DCs by $\Delta pksP$, $\Delta ayg1$ and $\Delta arp2$ conidia
94 was in part due to amorphous proteinaceous conidial surface with patchy rodlets or surface
95 exposed other cell wall component. $\Delta arp1$ conidia phenotype was intermediate between $\Delta arp2$

and $\Delta abr1$, whereas $\Delta abr1$, $\Delta abr2$ and WT conidia lack such material and have conidial surfaces covered with rodlets, which contribute for the masking of conidia recognition by the innate immune cells.

1. Material and Methods

2.1. Fungal strains and culture conditions

The melanin precursor strains $\Delta pksP$, $\Delta ayg1$, $\Delta arp2$, $\Delta arp1$, $\Delta abr1$, $\Delta abr2$ and the wild-type (WT) strain B5233 have been maintained in silica gel at J. Kwon-Chung's laboratory in NIH until use (6, 14, 15). All strains were cultivated on malt-agar (2%) medium at ambient temperature for at least 15-days before collecting the resting conidia. Conidia were harvested from the culture medium using 0.05% Tween-20 in water. Conidial suspensions were filtered on BD Falcons (BD Biosciences) to remove any mycelium. For immunolabeling and DC experiments, resting conidia were fixed with paraformaldehyde (PFA)-fixed (2.5% (v/v) PFA in PBS) for overnight at 4°C. The fixed conidia were subsequently washed three times with 0.1 M NH_4Cl and once with PBS-0.1% Tween-20.

2.2. Melanin extraction

The isolation of melanin from the WT conidia was performed as previously described (20, 21). After growing the fungus on malt-agar medium for 15-days at ambient temperature, conidia of each strain were collected in an aqueous 0.05% Tween-water. Briefly, Conidia were treated with a combination of proteolytic (proteinase K, Sigma) and glycohydrolytic (Glucanex, Novo) enzymes, denaturant (guanidine thiocyanate) and hot, concentrated HCl (6 M). This treatment resulted in an electron-dense layer similar in size and shape to the original conidial melanin layer without underlying cell components for which reason they were called “melanin ghosts” (20).

120 **2.3. *Extraction of the alkali soluble (AS) polysaccharide fraction from conidia***

121 Conidia were disrupted with 0.5 mm diameter glass beads in a FastPrep (MP Biomedicals). The
122 conidial cell wall fraction was recovered by centrifugation, washed with water then freeze-dried.
123 Dried cell wall fraction was boiled 50 mM Tris-HCl pH 7.4 containing 50 mM EDTA, 2% SDS
124 and 40 mM β -mercaptoethanol (10 min, twice) to get rid of proteins and extensively washed with
125 water so as to have cell wall polysaccharides. From the latter, the AS-fraction was extracted as
126 described earlier (22).

127

128 **2.4. *Extraction of conidial surface RodA protein (RodAp) involved in the rodlet formation***

129 The RodAp was extracted from the spore surface by incubating 10^9 dry conidia with 48% (v/v)
130 hydrofluoric acid (HF) for 72 h at 4°C (23). The contents were centrifuged (10,000 g, 10 min)
131 and the supernatant obtained was dried under N₂. The dried material was reconstituted in H₂O
132 and an aliquot was subjected to 15% (w/v) SDS-PAGE analysis and visualized by silver nitrate
133 staining.

134

135 **2.5. *Analysis of proteins on the conidial surface***

136 Conidia were incubated in 0.5 M NaCl solution for 2 h at room temperature at a ratio of 10^{10}
137 conidia per ml. The NaCl supernatant was recovered after centrifugation and directly subjected to
138 10% SDS-PAGE (w/v). 2D-gel electrophoretic analysis of the NaCl extract was carried out as
139 described previously with slight modifications (24, 25). A total amount of 50-100 μ g protein was
140 loaded onto IPG strips (11 cm, pH 3-7; GE Healthcare Life Sciences) by in-gel rehydration. After
141 equilibration of the IPG strips, SDS-gel electrophoresis was carried out using Criterion AnykD
142 TGX Stain-Free precast gels (Bio-RAD). Proteins were visualised by UV light and colloidal
143 Coomassie staining (Candiano2004). After scanning, gel images were analysed with the software

144 Delta 2D 4.3. (Decodon). Protein spots were excised and analysed by mass spectrometry using an
145 ultrafleXtreme MALDI-TOF/TOF device (Bruker Daltonics) as described (26).

146

147 ***2.6. Analysis of carbohydrate on the conidial surface by fluorescence microscopy***

148 The mannose moieties of glycoproteins on the resting conidial surface were labeled with ConA-
149 FITC (Sigma) at 0.1 mg/ml concentrations after incubating the resting conidia for 1 h at 37°C in
150 0.1 M carbonate buffer pH 9.6 containing 0.1% Tween-20. The hexosamines were labeled with
151 WGA-FITC at 0.1 mg/ml concentrations upon incubating the resting conidia for 1 h at the room
152 temperature in PBS containing 0.1% Tween-20. For immunolabeling, PFA-fixed conidia were
153 incubated with different antibodies as described previously (27). β -(1,3)-glucan was labeled with
154 Dectin-1 (Fc-dectin1 6 μ g/ml) followed by FITC conjugated GaHu-Fab2-human IgG (15 μ g/ml,
155 a kind gift from G. Brown, University of Aberdeen, Aberdeen, UK) (28).

156

157 ***2.7. Antibodies and reagents for human immunology***

158 Recombinant human (rh) GM-CSF and IL-4 were from Miltenyi Biotec (France). Fluorescein
159 isothiocyanate (FITC)-conjugated monoclonal antibodies (MAbs) to CD80; phycoerythrin (PE)-
160 conjugated MAbs to CD83 and CD86 were from BD Biosciences (France) and PE-conjugated
161 MAb to CD40 was from Becton Dickinson (France). Anti Thr202/Tyr204 phospho-ERK1/2, anti-
162 Thr180/Tyr182 phospho-p38 MAPK, antibodies were purchased from Cell Signaling Technology
163 (USA). Anti- β -actin antibody (AC-15) was from Sigma-Aldrich (USA).

164

165 ***2.8. Generation and culture of human dendritic cells***

166 Monocyte-derived DCs were generated as previously described (29, 30). Immature DCs (0.5×10^6
167 cells/well/ml) were cultured in the presence of GM-CSF and IL-4 (cytokines) alone; with

168 cytokines and PFA-fixed conidia of wild type or melanin mutants (1:1 ratio); or cytokines and 1
169 μg of melanin extracts; or cytokines and 1 μg of alkali soluble polysaccharide fraction of *A.*
170 *fumigatus* cell wall (positive control); or cytokines and NaCl extracts from 0.75×10^9 conidia for
171 48 hours. Cells were harvested and cell-free supernatants were stored at -80°C for cytokine
172 analysis. Cells were labeled with fluorochrome-conjugated MAbs for surface marker analysis by
173 using LSR II flow cytometry (BD Biosciences). Five thousand events were recorded for each
174 sample and data were analyzed by BD FACS DIVA software (BD Biosciences).

175

176 **2.9. Mixed lymphocyte reaction**

177 CD4^+ T cells were isolated from peripheral blood mononuclear cells of healthy donors using CD4
178 micro-beads (Miltenyi Biotec). DCs were washed extensively and were co-cultured with 1×10^5
179 responder CD4^+ T cells at DC:T cell ratios of 1:10, 1:20, 1:40 and 1:80. After 4 days, either cells
180 were harvested and cell-free supernatants were stored at -80°C for cytokine analysis or cells were
181 pulsed for 16-18 h with $0.5 \mu\text{Ci}$ of (^3H) thymidine. Radioactive incorporation was measured by
182 standard liquid scintillation counting. The proliferation of cells was measured as counts per
183 minute (cpm) (mean \pm SEM of quadruplicate values) after subtracting values of responder T cell
184 cultures alone.

185

186 **2.10. Measurement of cytokines**

187 Cytokines were quantified in cell-free culture supernatants using BD CBA Human Inflammation
188 kit and Human Th1/Th2 kits (BD Biosciences).

189

190 **2.11. Statistical analysis**

191 Two-sided, Student-t-test was used for the statistical analysis. $P < 0.05$ was considered as
192 significant (* $P < 0.05$, ** $P < 0.01$).

193

194 2.12. *Immunoblotting*

195 Immunoblotting was performed as described previously (31). DCs were washed with ice-cold
196 PBS in RIPA lysis buffer (50 mM Tris-HCl, pH 7.4, 1%NP-40, 0.25%Na-deoxycholate, 150mM
197 NaCl, 1mM EDTA, 1mM PMSF, 1 μ g/ml each aprotinin, leupeptin, pepstatin, 1mM Na_3VO_4 ,
198 1mM NaF). Equal amounts of proteins from the total cell lysates were subjected to SDS-PAGE
199 followed by transfer of proteins to polyvinylidene difluoride membranes. Membranes were
200 blocked in TBST buffer (0.02 M Tris-HCl (pH 7.5), 0.15 M NaCl and 0.1% Tween 20)
201 containing 5% non-fat dried milk and investigated with a primary antibody for overnight at 4°C.
202 After washing with TBST, membranes were incubated with HRP-conjugated secondary antibody
203 (Jackson immunologicals, USA). The blots were then developed with an enhanced
204 chemiluminescence detection system (Perkin Elmer, USA) as per manufacturer's instructions.

205

206 2.13. *Analysis of the conidial surface by atomic force microscopy (AFM)*

207 Conidial surfaces were analyzed by AFM, using a Multimode VIII instrument (Bruker, Santa
208 Barbara, CA). Sample immobilization was achieved by mechanically trapping living conidia into
209 porous polycarbonate membranes (it4ip SA, Belgium). After filtering a concentrated suspension
210 of cells, the membrane was rinsed with deionized water, carefully cut and attached to a metallic
211 puck using double-sided tape. Then the mounted sample was transferred to the AFM liquid cell
212 while avoid dewetting. Imagings were performed in contact mode under minimal applied force,
213 using oxide-sharpened microfabricated Si_3N_4 cantilevers (MSCT, Bruker) with a nominal spring
214 constant of 0.01 N/m. Force measurements were carried out by chemical force microscopy

(CFM) (32, 33) using gold tips (OMCL-TR4, Olympus, Tokyo, Japan), coated with hydrophobic thiols. To do so, cleaned tips were immersed for 12 h in 1 mM solutions of HS(CH₂)₁₁CH₃ (Sigma) in ethanol, rinsed and dried with N₂ prior to use. The cantilevers spring constants were measured by the thermal noise method (Picoforce, Bruker). Force curves were analyzed in order to determine the adhesion force between the conidia and the AFM tip. These adhesion forces were plotted as bright pixels, brighter colors indicating larger adhesion values. Data were processed using the commercial Nanoscope analysis (Bruker) and MATLAB softwares (The MathWorks, Natick, MA). For each strain, several images were taken on different conidia and force measurements were obtained in duplicate using different tips.

3. Results

3.1. *A. fumigatus* conidia from $\Delta pksP$, $\Delta ayg1$ and $\Delta arp2$ induce maturation and activation of human dendritic cells: Conidia from individual melanin biosynthetic pathways gene deletion mutants were used to study the maturation and activation of DCs. Melanin-mutant conidia deficient in the early steps of the biosynthetic pathway ($\Delta pksP$, $\Delta ayg1$ and $\Delta arp2$) induced maturation of DCs as demonstrated by the significantly enhanced expression of CD83 and co-stimulatory molecules CD86, CD80 and CD40 (Fig. 2) (34, 35). The $\Delta pksP$, $\Delta ayg1$ and $\Delta arp2$ conidia also stimulated a panel of DC-cytokines such as TNF- α , IL-1 β , IL-6 and IL-10 (Fig. 3). Upon vermeline biosynthesis, the subsequent downstream melanin biosynthetic pathway mutant conidia ($\Delta abr1$, $\Delta abr2$) behaved like the WT strain, becoming immunologically inert (Fig. 2, 3). The $\Delta arp1$ conidia presented an intermediate phenotype, as they induced only modest changes in the expression of co-stimulatory molecules of DCs and secretion of DC-cytokines (Figs. 2, 3).

238 **3.2. Melanin does not stimulate DC maturation:** As shown in the Figure 4, Melanin ghosts
239 from WT conidia did not induce DC maturation (Fig 4A). We further verified the lack of
240 activation of DCs by analyzing the intracellular signaling pathways and ability of DCs to induce
241 T cell proliferation and cytokines (Fig. 4B-D). We show that melanin ghost failed to
242 phosphorylate p38 MAPK and ERK thus confirming the immunological inert nature of melanin
243 (Fig. 4B). The lack of activation of DCs by WT ghost extract was also reflected in the inability of
244 WT ghost extract-treated DCs to promote T cell proliferation (Fig. 4C) and T cell cytokines IL-2,
245 IFN- γ and IL-5 (Fig. 4D). On the contrary, the AS polysaccharide fraction (rich in $\alpha(1,3)$ -glucan)
246 of the *A. fumigatus* cell wall, used as a positive control, induced maturation of DCs, activation of
247 intracellular signaling pathways and promoted DC-mediated T cell proliferation and cytokine
248 production (Fig. 4A-D). Taken together, these data indicated that conidial surface melanin, either
249 *in situ* or in the extracted form (melanin ghosts), failed to stimulate DC activation and cytokine
250 production.

251

252 **3.3. The surface rodlet layer is masked by an amorphous hydrophilic layer:** To investigate
253 if the structural modifications in the $\Delta pksP$, $\Delta ayg1$, $\Delta arp2$ and $\Delta arp1$ conidia could be
254 responsible for stimulating the DCs, conidial surfaces were imaged by atomic force microscopy
255 (AFM) (36, 37) (Fig. 5A-O). Rather than using an incident beam as in classical microscopy,
256 AFM probes the small forces acting on the sample surface (37). Three-dimensional images are
257 generated in buffer by scanning a sharp tip over the cell surface while sensing the interaction
258 force between the tip and the surface. Originally invented for topographic imaging, AFM has
259 evolved into a multifunctional molecular toolkit, enabling researchers not only to observe
260 structural details of cells to near molecular resolution (36, 38), but also to measure their

261 biophysical properties and interactions (39-41). In contrast to the WT conidia that are covered
262 with rodlet structure (30, 42) (Fig. 5M-O), the $\Delta pksP$ mutant conidial surface was amorphous
263 without organized rodlet structure (Fig. 5A-C). Some patches of organized rodlet layers were
264 observed on the $\Delta ayg1$ conidial surface (Fig. 5D-F) and their percentage increased on the $\Delta arp2$
265 conidia (Fig. 5G-I), to finally cover almost all the surface of $\Delta arp1$ conidia (Fig. 5J-L). However,
266 the rodlet layer on $\Delta arp1$ conidia appeared to be less compact and less organized than that of the
267 WT conidia (Fig. 5M and O). The mutants of further down-stream melanin biosynthetic pathway
268 genes, $\Delta abr1$ and $\Delta abr2$, presented organized and compact rodlets on the entire surface of their
269 conidia, similar to WT conidia (data not shown).

270

271 To investigate if RodAp (responsible for the formation of rodlet layer on the conidial surface) is
272 still present on the $\Delta pksP$ mutant conidial surface, all the mutant conidia as well as the WT
273 conidia were treated with HF (30). RodAp could be extracted from the $\Delta pksP$, other melanin
274 mutants and the WT conidia. Their SDS-PAGE profiles (Fig. 6) showed that two bands of RodAp
275 classically seen in the HF extracts of conidia were present in all the melanin pathway mutants and
276 WT conidia (30). A band at 18 kDa could also be observed in $\Delta pksP$, $\Delta ayg1$ and $\Delta arp2$ HF
277 extracts (Fig. 6). Mass spectrometry (MS) and MS/MS analysis showed that this 18 kDa protein
278 corresponds to the Aspfl antigen, suggesting the loose architecture of rodlets in these mutants.
279 These data confirmed AFM observations that the RodAp were present but hidden by an
280 amorphous material on the surface of $\Delta pksP$, $\Delta ayg1$ and $\Delta arp2$ mutant conidia.

281

282 Because, the presence of this amorphous material covers the hydrophobic rodlets, we asked
283 whether the observed surface changes correlated with differences in the conidial hydrophobic
284 adhesive properties. To understand this, we mapped and quantified the nanoscale adhesion

properties of WT and $\Delta pksP$ mutant conidia by AFM with hydrophobic tips. The presence of this unorganized material on the $\Delta pksP$ mutant conidial surface was associated with a dramatic reduction in their conidial surface hydrophobicity (Fig. 7). For the WT, force-distance curves recorded across the cell surface revealed large adhesion forces, ranging from 0.2 to 6 nN (Figs. 7M-O). In contrast, structural changes in $\Delta pksP$ conidia caused profound modifications in the cell surface physico-chemical properties (Figs. 7A-C). Force-distance curves and force maps showed the absence of adhesion forces over the entire surface of the $\Delta pksP$ mutant conidia, indicating that this mutant is hydrophilic. The adhesion force of the other mutants of the melanin pathway increased with the rank of the mutant in the pathway, from a low adhesion with the $\Delta pksP$ and $\Delta ayg1$ conidia (Figs. 7A-F), to a maximal adhesion with WT conidia (Figs. 7M-O). The low adhesion capacities of the $\Delta pksP$, $\Delta ayg1$ and $\Delta arp2$ conidia indicated a modification of the cell surface hydrophobicity that could have influenced conidial recognition by DCs.

3.4 Proteins are present in the amorphous hydrophilic layer of $\Delta pksP$ and $\Delta ayg1$ mutant conidia: We then investigated the chemical nature of the amorphous layer present on the surface of $\Delta pksP$, $\Delta ayg1$ and $\Delta arp2$ mutant conidia. A strong labeling with ConA was observed only with the $\Delta pksP$ conidia, suggesting that its surface layer is rich in glyco-conjugates. However, labeling with ConA was either low or negative in other melanin mutants including $\Delta ayg1$ and $\Delta arp2$, and WT conidia (Fig. 8; data not shown). The surface amorphous material could be extracted by incubating mutant conidia (mutants for the initial steps of melanin biosynthesis) with 0.5 M NaCl for 2 h and they were positive for protein test, suggesting the presence of glycoproteins in this conidial surface amorphous material. As shown in Figure 9, the amount of proteins present in the extract was very high in $\Delta pksP$ mutant followed by $\Delta ayg1$. Extract from $\Delta pksP$ contained 53 μ g of proteins per 3×10^9 conidia whereas $\Delta ayg1$ conidial extract contained

309 12 µg of proteins. The surface extracts of other mutants conidia i.e., *Δarp2* and *Δarp1* contained
 310 3.8 µg proteins while in *Δabr1*, *Δabr2* and WT extracts, the amount of proteins was too low to
 311 detect. These results thus indicate that smaller amounts of proteins on the surface layer of *Δayg1*,
 312 *Δarp2* and *Δarp1* conidia reflected in the low or negative ConA-FITC staining of these conidia.
 313 Extracted protein mixture of *ΔpksP* was subjected to proteomic analysis. Forty-two proteins
 314 were identified in the extract and *in-silico* analysis of these proteins by SigPred
 315 (<http://www.cbs.dtu.dk/services/SignalP/>) and CADRE ([http://www.cadre-](http://www.cadre-genomes.org.uk/Aspergillus_fumigatus/)
 316 [genomes.org.uk/Aspergillus_fumigatus/](http://www.cadre-genomes.org.uk/Aspergillus_fumigatus/)) revealed that all of them had a signal peptide (Table 1).
 317 Extracellular proteins, normally secreted during the vegetative growth of *A. fumigatus*, such as
 318 Cat1p, Exg1p and ExoG2p, Asp1p, ChiB1 were identified in the NaCl extract of *ΔpksP* resting
 319 conidia (43-46). Nine of forty-one proteins were glycosylhydrolases. RodAp was also identified
 320 in the NaCl extract. Other proteins, such as proteasome components, translation elongation
 321 factors, pyruvate dehydrogenases, adenosine deaminase, protein disulfide isomerase normally
 322 found in intracellular compartments, were present in very low amounts as they were identified
 323 only once or twice in the proteomic survey.
 324
 325 In order to determine whether the proteins present on the surface of *ΔpksP* and *Δayg1* conidia are
 326 responsible for the activation of DC by these mutant conidia, we incubated DCs with the NaCl
 327 extract of *ΔpksP*, *Δayg1*, *Δarp2*, *Δarp1* and WT mutant conidia. As expected, NaCl extract of
 328 *ΔpksP* and *Δayg1* induced maturation of DCs, whereas the NaCl extracts of *Δarp2*, *Δarp1* and
 329 WT did not (Fig. 10A-C). These results demonstrated that the surface protein layer was
 330 responsible at least in part for the induction of DC maturation following incubation of cells with
 331 resting conidia of *ΔpksP* and *Δayg1*. However, the amount of proteins present on the surface of
 332 *Δarp2* and *Δarp1* was too low to stimulate DC cells (Fig. 10). Although NaCl extracts from the

333 *ΔpksP* and *Δayg1* mutant conidial surfaces induced maturation of the DCs based on the
334 phenotype analysis of cells (Fig. 10), they did not induce production of the cytokines such as IL-
335 1 β , IL-10 or IL-6 (data not shown). The level of production of above cytokines was on par with
336 control DCs. These data suggest that signals provided by NaCl extracts of *ΔpksP* and *Δayg1*
337 mutant conidia were not sufficient to induce functional activation of the DCs. On the other hand,
338 *ΔpksP*, *Δayg1* and *Δarp2* mutant conidia induce various DC cytokines, which could be due to the
339 exposure of cell wall polysaccharides on their conidial surfaces.

340

341 **3.5 Glucosamine-containing components are exposed at the *ΔpksP*, *Δayg1* and *Δarp2***

342 **conidial surfaces:** To check if any structural cell wall modification occurred and was responsible
343 for DC activation by *ΔpksP*, *Δayg1* and *Δarp2* conidia, we labeled mutant and WT conidia with
344 the β -(1,3)-glucan receptor Dectin-1 and with the glucosamine (GlcN) recognizing lectin wheat-
345 germ agglutinin (WGA). Mutants and WT conidia did not bind to Dectin-1 (data not shown),
346 suggesting that β -(1,3)-glucans were not exposed at the conidial surfaces. However, *ΔpksP*,
347 *Δayg1* and *Δarp2* were positive for WGA-FITC (Fig. 11), whereas *Δabr1*, *Δabr2* and WT
348 conidia were 3 to 9% WGA-FITC positive (Fig. 11). In line with partial stimulation of DCs,
349 *Δarp1* presented an intermediate phenotype: about 40% conidia were WGA-positive. These
350 results suggested that conidia with uniform exposure of glucosamine-containing components on
351 the surface (in cases of *ΔpksP*, *Δayg1* and *Δarp2* mutant conidia) were able to induce DC
352 activation whereas conidia with low level of exposure of GlcN-content on the surface did not
353 stimulate DC cells (*Δabr1*, *Δabr2* and WT). When GlcN-exposure was intermediate as in *Δarp1*
354 conidia, such conidia were able to induce partial activation of DCs.

355

356 Consequently, the absence of melanin or at least of the intermediate scytalone increased
357 permeability of the conidia to secreted proteins which otherwise secreted normally during
358 conidial germination, and exposed the GlcN-polymers on the conidial surfaces. Proteins and
359 GlcN-polymers were responsible for the DCs activation following incubation of cells with
360 $\Delta pksP$, $\Delta ayg1$ and $\Delta arp2$ conidia. The $\Delta abr1$ and $\Delta abr2$ conidia were immunologically inert like
361 their WT counterparts whereas $\Delta arp1$ presented an intermediate phenotype.

362

363 **4. Discussion**

364 In fungal biology, melanin pigments are attributed with a variety of beneficial function including
365 protection against exogenous stress, UV-irradiation and host defense mechanisms including
366 reactive oxygen species, lytic enzymes and antimicrobial peptides (47) and hence considered to
367 be one of the fungal virulence factors (48). Melanin, being extracellular, also contributes to the
368 fungal spore structure (5). In *A. fumigatus*, the melanin biosynthesis is reported to require a
369 cluster of six genes (6, 13, 14). In the present study, for the first time we show the effect of
370 deletion of individual genes from the melanin biosynthetic gene cluster on the respective conidial
371 surface morphology and the consequent immune responses to the mutant conidia.

372

373 The mutant conidia with deletion in one of the first three genes of the melanin pathway, $\Delta pksP$,
374 $\Delta ayg1$ and $\Delta arp2$, stimulated the maturation and elicited production of IL-6, IL-1 β and TNF- α
375 and IL-10 cytokines by DCs, whereas $\Delta abr1$, $\Delta abr2$ and WT conidia were not immunogenic. The
376 $\Delta arp1$ mutant presented an intermediate phenotype as it induced partial activation of DCs.
377 Melanin as such were immunologically inert as the melanin ghost extracted from the WT conidia
378 failed to activate DCs. These results suggested that the surface of $\Delta pksP$, $\Delta ayg1$, $\Delta arp2$ resting

379 conidia are covered with specific common compounds which are rare in *Δarp1* and are
380 responsible for the maturation of DCs.

381

382 The major obvious phenotypes of the *ΔpksP Δayg1* and *Δarp2* resting conidia were the absence
383 or very few patches of rodlets at the surface. Although the rodlets that immune-silence the resting
384 conidia were present in the above mutant conidia, the masking of rodlets by an amorphous and
385 hydrophilic layer enabled resting conidia to be immunogenic (24, 49). A few patches of
386 amorphous and hydrophilic layer could also be observed on *Δarp1* conidial surface. When
387 downstream genes of the DHN-melanin pathway were deleted, the appearance of the rodlets and
388 the hydrophobicity of the conidia increased. Previous studies demonstrated that deletion of *PKSP*
389 and *ARP2* correlated with a decreased ability to bind laminin on the conidial surface (10). This
390 result is explained by the low hydrophobicity of the conidia, which reduced the electronegative
391 charge, required for laminin binding.

392

393 The amorphous and hydrophilic layer is composed of GlcN-containing components and deposited
394 ConA-positive proteins mostly in *ΔpksP*. These proteins were analyzed in the *ΔpksP* mutant and
395 their identification showed that they are usually secreted during vegetative growth. Most
396 hydrolases (such as β-1,3-glucosidases, β-N-acetylhexosaminidase, mannosidase), catalase,
397 Aspfl, Asp-hemolysin, and chitinase found in the amorphous surface layer of the resting *ΔpksP*
398 conidia were usually identified during mycelial growth in a protein-based medium (43-46). Their
399 presence on the surface of the resting conidia of *ΔpksP* and *Δayg1* is explained by modifications
400 of the ionic strength of the hydrophobin layer resulting from the absence of melanin or at least the
401 YWA1, a melanin biosynthetic intermediate which is synthesized by the combined activities of
402 PksPp and Ayg1p. The easy removal of these hydrophilic glycoproteins by 0.5 M NaCl suggested

403 that they adhered to the conidial cell wall through electrostatic binding. These surface proteins in
404 the conidial amorphous layers were responsible for the DC maturation and cytokine production.
405 Interestingly, cell wall structural modifications resulting from the absence of α -(1,3) glucan as in
406 *A. fumigatus* $\Delta ags1\Delta ags2\Delta ags3$ (Δags) mutant also gave the similar conidial phenotype, a
407 hydrophilic protein layer on the surface of the conidia which stimulated the host defense
408 reactions (24). However, the composition of proteins in this amorphous layer in the triple Δags
409 and $\Delta pksP$ deletion mutants was not the same, suggesting defined cell wall permeability defects
410 due to the deletion of different cell wall component biosynthetic genes. When the melanin
411 synthesis pathway was blocked more downstream by gene deletion, fewer proteins were able to
412 cross the conidial cell wall. Of note, DC cytokine production was less for $\Delta pksP$ than for $\Delta ayg1$
413 and $\Delta arp2$ mutant conidia (Fig. 3). This result suggests that glycoproteins were less stimulatory
414 than GlcN-residues present on the surfaces of the $\Delta pksP$, $\Delta ayg1$ and $\Delta arp2$ mutant conidia, and
415 that these GlcN-residues are less exposed on $\Delta pksP$ mutant surface due to the higher amount of
416 glycoproteins in this mutant.

417

418 The presence of GlcN-residues on the surfaces of the $\Delta pksP$ $\Delta ayg1$ and $\Delta arp2$ mutant conidia
419 could be explained by the unmasking of cell wall chitin due to the absence of melanin. The
420 hexosamines present in the conidial cell wall were composed of long chains of fibrillar water
421 insoluble chitin, amorphous and soluble chitin oligosaccharides (containing 10-15 *N*-acetyl-
422 glucosamine) and deacetylated chitin (chitosan) (Beauvais *et al*, unpublished results). Previous
423 studies on different sized chitin polymers have shown that >70 μm chitin polymers were
424 immunologically inert with murine macrophages, while both intermediate-sized (40–70 μm) and
425 <40 μm chitin polymers stimulated TNF elaboration by macrophages (50), and only <40 μm
426 chitin polymers induced IL-10 production. Small particles of chitosan were even better

macrophage immune-stimulators. Chitosan of less than 20 μm elicited the most IL-1 β from bone marrow-derived macrophages (50). Although several chitin-binding proteins have been identified in mammalian cells, no chitin receptor had thus far been identified so far. A recent study on recognition of innate immune cells by *Candida albicans* chitin revealed that though there was no direct dectin-1 and chitin binding, chitin was capable of blocking dectin-1 mediated immune responses (51). Similarly, these small and/or deacetylated chitins were likely unmasked on the surface of the first three melanin mutants and were responsible for the DC maturation. Such an unmasking phenomenon was reported in chitin synthase mutants ΔcsmA and ΔcsmB , wherein the deletion of two of the chitin synthase genes (*CSMA* and *CSMB*) in *A. fumigatus* resulted in the increased exposure of WGA-positive components on the conidial surfaces (42). The ΔcsmA conidial surface was also amorphous and ConA-positive; however, ConA-positive materials were not glycoproteins, rather due to the exposure of mannan-containing polymers. This further confirms the differential permeability defects due to the deletion of specific cell wall component biosynthetic genes.

Chai and co-workers (9) also demonstrated that melanin purified from WT conidia was also poorly immunogenic for the stimulation of cytokines by peripheral blood mononuclear cells. On the other hand, as seen in our study, ΔpksP conidia elicited significantly higher cytokine production, such as IL-10, IL-6 and TNF- α . They found that blockage of dectin-1 with laminarin reduced the cytokine production in response to ΔpksP conidia, which could be correlated with WGA-FITC positivity of ΔpksP , Δayg1 and Δarp2 mutant conidia and the observations that chitin can influence dectin-1 mediated immune responses (51). Jahn and co-workers (52) observed that macrophage phagocytosis and intracellular killing was significantly higher with ΔpksP conidia than WT conidia. Thywissen and co-workers (18) showed that inside the

451 phagolysosome, WT conidial DHN-melanin was responsible for the inhibition of the
452 phagolysosomal acidification of mouse and human macrophages and neutrophils. The $\Delta pksP$
453 conidia, in contrast, were located in an acidic environment in the phagolysosome, which
454 coincides with more effective killing of these conidia. The percentage of $\Delta ayl1$, $\Delta arp2$ and
455 $\Delta abr2$ conidia were lower in acidified-phagolysosomes than $\Delta pksP$ conidia, but higher compared
456 to the WT conidia. These results show that melanin intermediates formed by the downstream
457 biosynthetic pathway increase the conidial protection. However, the final product, the DHN-
458 melanin, was important for the maximal protection as it facilitates the formation of a complete
459 surface rodlet layer that hides conidia from their immediate recognition by the immune system.

460

461 **5. Conclusions**

462 The absence of at least the scytalone intermediate of DHN melanin is responsible for structural
463 and chemical modifications of the cell surface, which will have an obvious impact on the immune
464 response of the host towards the corresponding mutant. Our results also show that melanin is
465 essential to acquire the right surface properties with precise charge and hydrophobicity that are
466 necessary to have immunologically inert conidia due to an exposed rodlet layer.

467

468 **Acknowledgements:** Maria Pötsch is acknowledged for excellent technical support.

469

470 **Funding:** The work reported was partly supported by the Aviesan grant BA-P1-09 *Aspergillus*.
471 Research in the Unité des *Aspergillus*, Institut Pasteur and Institut National de la Santé et de la
472 Recherche Médicale Unité 1138 was supported by European Community's Seventh Framework
473 Programme [FP7/2007-2013] under Grant Agreement No: 260338 ALLFUN and ANR-10-
474 BLAN-1309 HYDROPHOBIN. Work at the Université catholique de Louvain was supported by

475 the National Fund for Scientific Research (FNRS), the Université catholique de Louvain (Fonds
476 Spéciaux de Recherche), the Federal Office for Scientific, Technical and Cultural Affairs
477 (Interuniversity Poles of Attraction Programme), and the Research Department of the
478 Communauté française de Belgique (Concerted Research Action). The funders had no role in
479 study design, data collection and analysis, decision to publish, or preparation of the manuscript.

480

481 **Competing Interests:** The authors have declared that no competing interests exist.

482

483 **References:**

- 484 1. **Rosa LH, Almeida Vieira Mde L, Santiago IF, Rosa CA.** 2010. Endophytic fungi
485 community associated with the dicotyledonous plant *Colobanthus quitensis* (Kunth)
486 Bartl. (Caryophyllaceae) in Antarctica. *FEMS Microbiol. Ecol.* **73**:178-189.
- 487 2. **Zalar P, Novak M, de Hoog GS, Gunde-Cimerman N.** 2011. Dishwashers--a man-
488 made ecological niche accommodating human opportunistic fungal pathogens. *Fungal*
489 *Biol.* **115**:997-1007.
- 490 3. **Ngamskulrungrroj P, Price J, Sorrell T, Perfect JR, Meyer W.** 2011. *Cryptococcus*
491 *gattii* virulence composite: candidate genes revealed by microarray analysis of high and
492 less virulent Vancouver island outbreak strains. *PLoS One.* **6**:e16076.
- 493 4. **Volling K, Thywissen A, Brakhage AA, Saluz HP.** 2011. Phagocytosis of melanized
494 *Aspergillus* conidia by macrophages exerts cytoprotective effects by sustained PI3K/Akt
495 signalling. *Cell. Microbiol.* **13**:1130-1148.
- 496 5. **Jahn B, Koch A, Schmidt A, Wanner G, Gehringer H, Bhakdi S, Brakhage AA.**
497 1997. Isolation and characterization of a pigmentless-conidium mutant of *Aspergillus f*
498 *umigatus* with altered conidial surface and reduced virulence. *Infect. Immun.*
499 **65**:5110-5117.
- 500 6. **Tsai HF, Wheeler MH, Chang YC, Kwon-Chung KJ.** 1999. A developmentally
501 regulated gene cluster involved in conidial pigment biosynthesis in *Aspergillus fumigatus*.
502 *J. Bacteriol.* **181**:6469-6477.
- 503 7. **Schmaler-Ripcke J, Sugareva V, Gebhardt P, Winkler R, Knienmeyer O, Heinekamp**
504 **T, Brakhage AA.** 2009. Production of pyomelanin, a second type of melanin, via the
505 tyrosine degradation pathway in *Aspergillus fumigatus*. *Appl. Environ. Microbiol.*
506 **75**:493-503.
- 507 8. **Eisenman HC, Casadevall A.** 2012. Synthesis and assembly of fungal melanin. *Appl.*
508 *Microbiol. Biotechnol.* **93**:931-940.
- 509 9. **Chai LY, Netea MG, Sugui J, Vonk AG, van de Sande WW, Warris A, Kwon-Chung**
510 **KJ, Kullberg BJ.** 2010. *Aspergillus fumigatus* conidial melanin modulates host cytokine
511 response. *Immunobiology* **215**:915-920.
- 512 10. **Pihet M, Vandeputte P, Tronchin G, Renier G, Saulnier P, Georgeault S, Mallet R,**
513 **Chabasse D, Symoens F, Bouchara JP.** 2009. Melanin is an essential component for the
514 integrity of the cell wall of *Aspergillus fumigatus* conidia. *BMC Microbiol.* **9**:177.
- 515 11. **Keller S, Macheleidt J, Scherlach K, Schmaler-Ripcke J, Jacobsen ID, Heinekamp**
516 **T, Brakhage AA.** 2011. Pyomelanin formation in *Aspergillus fumigatus* requires HmgX
517 and the transcriptional activator HmgR but is dispensable for virulence. *PLoS One.*
518 **6**:e26604.

- 519 12. **Sugareva V, Hartl A, Brock M, Hubner K, Rohde M, Heinekamp T, Brakhage AA.** 2006. Characterisation of the laccase-encoding gene *abr2* of the dihydroxynaphthalene-like melanin gene cluster of *Aspergillus fumigatus*. *Arch. Microbiol.* **186**:345-355.
- 520
- 521
- 522 13. **Tsai HF, Fujii I, Watanabe A, Wheeler MH, Chang YC, Yasuoka Y, Ebizuka Y, Kwon-Chung KJ.** 2001. Pentaketide melanin biosynthesis in *Aspergillus fumigatus* requires chain-length shortening of a heptaketide precursor. *J. Biol. Chem.* **276**:29292-29298.
- 523
- 524
- 525
- 526 14. **Tsai HF, Washburn RG, Chang YC, Kwon-Chung KJ.** 1997. *Aspergillus fumigatus* *arp1* modulates conidial pigmentation and complement deposition. *Mol. Microbiol.* **26**:175-183.
- 527
- 528
- 529 15. **Fujii I, Yasuoka Y, Tsai HF, Chang YC, Kwon-Chung KJ, Ebizuka Y.** 2004. Hydrolytic polyketide shortening by *ayg1p*, a novel enzyme involved in fungal melanin biosynthesis. *J. Biol. Chem.* **279**:44613-44620.
- 530
- 531
- 532 16. **Langfelder K, Jahn B, Gehringer H, Schmidt A, Wanner G, Brakhage AA.** 1998. Identification of a polyketide synthase gene (*pksP*) of *Aspergillus fumigatus* involved in conidial pigment biosynthesis and virulence. *Med. Microbiol. Immunol.* **187**:79-89.
- 533
- 534
- 535 17. **Slesiona S, Gressler M, Mihlan M, Zaehle C, Schaller M, Barz D, Hube B, Jacobsen ID, Brock M.** 2012. Persistence versus escape: *Aspergillus terreus* and *Aspergillus fumigatus* employ different strategies during interactions with macrophages. *PLoS One.* **7**:e31223.
- 536
- 537
- 538
- 539 18. **Thywissen A, Heinekamp T, Dahse HM, Schmalzer-Ripcke J, Nietzsche S, Zipfel PF, Brakhage AA.** 2011. Conidial Dihydroxynaphthalene Melanin of the Human Pathogenic Fungus *Aspergillus fumigatus* Interferes with the Host Endocytosis Pathway. *Front. Microbiol.* **2**:96.
- 540
- 541
- 542
- 543 19. **Luther K, Torosantucci A, Brakhage AA, Heesemann J, Ebel F.** 2007. Phagocytosis of *Aspergillus fumigatus* conidia by murine macrophages involves recognition by the dectin-1 beta-glucan receptor and Toll-like receptor 2. *Cell. Microbiol.* **9**:368-381.
- 544
- 545
- 546 20. **Rosas AL, Nosanchuk JD, Gomez BL, Edens WA, Henson JM, Casadevall A.** 2000. Isolation and serological analyses of fungal melanins. *J. Immunol. Methods.* **244**:69-80.
- 547
- 548 21. **Youngchim S, Morris-Jones R, Hay RJ, Hamilton AJ.** 2004. Production of melanin by *Aspergillus fumigatus*. *J. Med. Microbiol.* **53**:175-181.
- 549
- 550 22. **Beauvais A, Maubon D, Park S, Morelle W, Tanguy M, Huerre M, Perlin DS, Latgé JP.** 2005. Two $\alpha(1-3)$ glucan synthases with different functions in *Aspergillus fumigatus*. *Appl. Environ. Microbiol.* **71**:1531-1538.
- 551
- 552
- 553 23. **Aimanianda V, Clavaud C, Simenel C, Fontaine T, Delepierre M, Latgé JP.** 2009. Cell wall beta-(1,6)-glucan of *Saccharomyces cerevisiae*: structural characterization and in situ synthesis. *J. Biol. Chem.* **284**:13401-13412.
- 554
- 555
- 556 24. **Beauvais A, Bozza S, Knemeyer O, Formosa C, Balloy V, Henry C, Roberson RW, Dague E, Chignard M, Brakhage AA, Romani L, Latgé JP.** 2013. Deletion of the $\alpha(1,3)$ -Glucan Synthase Genes Induces a Restructuring of the Conidial Cell Wall Responsible for the Avirulence of *Aspergillus fumigatus*. *PLoS Pathog.* **9**: e1003716..
- 557
- 558
- 559

- 560 25. **Kniemeyer O, Lessing F, Scheibner O, Hertweck C, Brakhage AA.** 2006.
561 Optimisation of a 2-D gel electrophoresis protocol for the human-pathogenic fungus
562 *Aspergillus fumigatus*. *Curr. Genet.* **49**:178-189.
- 563 26. **Muller S, Baldin C, Groth M, Guthke R, Kniemeyer O, Brakhage AA, Valiante V.**
564 2012. Comparison of transcriptome technologies in the pathogenic fungus *Aspergillus*
565 *fumigatus* reveals novel insights into the genome and MpkA dependent gene expression.
566 *BMC Genomics.* **13**:519.
- 567 27. **Lamarre C, Beau R, Balloy V, Fontaine T, Wong Sak Hoi J, Guadagnini S, Berkova**
568 **N, Chignard M, Beauvais A, Latgé JP.** 2009. Galactofuranose attenuates cellular
569 adhesion of *Aspergillus fumigatus*. *Cell. Microbiol.* **11**:1612-1623.
- 570 28. **Steele C, Rapaka RR, Metz A, Pop SM, Williams DL, Gordon S, Kolls JK, Brown**
571 **GD.** 2005. The beta-glucan receptor dectin-1 recognizes specific morphologies of
572 *Aspergillus fumigatus*. *PLoS Pathog.* **1**:e42.
- 573 29. **Bansal K, Sinha AY, Ghorpade DS, Togarsimalemath SK, Patil SA, Kaveri SV,**
574 **Balaji KN, Bayry J.** 2010. Src homology 3-interacting domain of Rv1917c of
575 *Mycobacterium tuberculosis* induces selective maturation of human dendritic cells by
576 regulating PI3K-MAPK-NF-kappaB signaling and drives Th2 immune responses. *J. Biol.*
577 *Chem.* **285**:36511-36522.
- 578 30. **Aimanianda V, Bayry J, Bozza S, Kniemeyer O, Perruccio K, Elluru SR, Clavaud C,**
579 **Paris S, Brakhage AA, Kaveri SV, Romani L, Latgé JP.** 2009. Surface hydrophobin
580 prevents immune recognition of airborne fungal spores. *Nature* **460**:1117-11121.
- 581 31. **Bansal K, Elluru SR, Narayana Y, Chaturvedi R, Patil SA, Kaveri SV, Bayry J,**
582 **Balaji KN.** 2010. PE_PGRS antigens of *Mycobacterium tuberculosis* induce maturation
583 and activation of human dendritic cells. *J. Immunol.* **184**:3495-3504.
- 584 32. **Alsteens D, Dague E, Rouxhet PG, Baulard AR, Dufrene YF.** 2007. Direct
585 measurement of hydrophobic forces on cell surfaces using AFM. *Langmuir.* 2007
586 **23**:11977-11979.
- 587 33. **Dufrene YF.** 2008. Atomic force microscopy and chemical force microscopy of
588 microbial cells. *Nat Protoc.* **3**:1132-1138.
- 589 34. **Banchereau J, Steinman RM.** 1998. Dendritic cells and the control of immunity. *Nature*
590 **392**:245-252.
- 591 35. **Cella M, Scheidegger D, Palmer-Lehmann K, Lane P, Lanzavecchia A, Alber G.**
592 1996. Ligation of CD40 on dendritic cells triggers production of high levels of
593 interleukin-12 and enhances T cell stimulatory capacity: T-T help via APC activation. *J.*
594 *Exp. Med.* **184**:747-752.
- 595 36. **Dufrene YF, Boonaert CJ, Gerin PA, Asther M, Rouxhet PG.** 1999. Direct probing of
596 the surface ultrastructure and molecular interactions of dormant and germinating spores of
597 *Phanerochaete chrysosporium*. *J. Bacteriol.* **181**:5350-5354.
- 598 37. **Dufrene YF.** 2004. Using nanotechniques to explore microbial surfaces. *Nat. Rev.*
599 *Microbiol.* **2**:451-460.

- 600 38. **Andre G, Kulakauskas S, Chapot-Chartier MP, Navet B, Deghorain M, Bernard E,**
601 **Hols P, Dufrêne YF.** 2010. Imaging the nanoscale organization of peptidoglycan in
602 living *Lactococcus lactis* cells. *Nat. Commun.* **1**:27.
- 603 39. **Alsteens D, Trabelsi H, Soumillion P, Dufrêne YF.** 2013. Multiparametric atomic force
604 microscopy imaging of single bacteriophages extruding from living bacteria. *Nat.*
605 *Commun.* **4**:2926.
- 606 40. **Beaussart A, Alsteens D, El-Kirat-Chatel S, Lipke PN, Kucharikova S, Van Dijck P,**
607 **Dufrêne YF.** 2012. Single-molecule imaging and functional analysis of Als adhesins and
608 mannans during *Candida albicans* morphogenesis. *ACS Nano* **6**:10950-10964.
- 609 41. **Dague E, Alsteens D, Latgé JP, Verbelen C, Raze D, Baulard AR, Dufrêne YF.** 2007.
610 Chemical force microscopy of single live cells. *Nano Lett.* **7**:3026-3030.
- 611 42. **Alsteens D, Aïmanianda V, Hegde P, Pire S, Beau R, Bayry J, Latgé JP, Dufrêne**
612 **YF.** 2013. Unraveling the nanoscale surface properties of chitin synthase mutants of
613 *Aspergillus fumigatus* and their biological implications. *Biophys. J.* **105**:320-327.
- 614 43. **Alcazar-Fuoli L, Clavaud C, Lamarre C, Aïmanianda V, Seidl-Seiboth V, Mellado**
615 **E, Latgé JP.** 2011. Functional analysis of the fungal/plant class chitinase family in
616 *Aspergillus fumigatus*. *Fungal Genet. Biol.* **48**:418-429.
- 617 44. **Singh B, Oellerich M, Kumar R, Kumar M, Bhadoria DP, Reichard U, Gupta VK,**
618 **Sharma GL, Asif AR.** 2010. Immuno-reactive molecules identified from the secreted
619 proteome of *Aspergillus fumigatus*. *J. Proteome Res.* **9**:5517-5529.
- 620 45. **Sriranganadane D, Waridel P, Salamin K, Reichard U, Grouzmann E, Neuhaus JM**
621 **Quadroni M, Monod M.** 2010. *Aspergillus* protein degradation pathways with different
622 secreted protease sets at neutral and acidic pH. *J. Proteome Res.* **9**:3511-3519.
- 623 46. **Wartenberg D, Lapp K, Jacobsen ID, Dahse HM, Kniemeyer O, Heinekamp T,**
624 **Brakhage AA.** 2011. Secretome analysis of *Aspergillus fumigatus* reveals Asp-hemolysin
625 as a major secreted protein. *Int. J. Med. Microbiol.* **301**:602-611.
- 626 47. **Heinekamp T, Thywissen A, Macheleidt J, Keller S, Valiante V, Brakhage AA.** 2012.
627 *Aspergillus fumigatus* melanins: interference with the host endocytosis pathway and
628 impact on virulence. *Front. Microbiol.* **3**:440.
- 629 48. **Buskirk AD, Templeton SP, Nayak AP, Hettick JM, Law BF, Green BJ, Beezhold**
630 **DH.** 2014. Pulmonary immune responses to *Aspergillus fumigatus* in an
631 immunocompetent mouse model of repeated exposures. *J Immunotoxicol.* **11**:180-189.
- 632 49. **Jimenez-Ortigosa C, Aïmanianda V, Muszkieta L, Mouyna I, Alsteens D, Pire S,**
633 **Beau R, Krappmann S, Beauvais A, Dufrêne YF, Roncero C, Latgé JP.** 2012. Chitin
634 synthases with a myosin motor-like domain control the resistance of *Aspergillus*
635 *fumigatus* to echinocandins. *Antimicrob. Agents Chemother.* **56**:6121-6131.
- 636 50. **Bueter CL, Lee CK, Rathinam VA, Healy GJ, Taron CH, Specht CA, Levitz SM.**
637 2011. Chitosan but not chitin activates the inflammasome by a mechanism dependent
638 upon phagocytosis. *J. Biol. Chem.* **286**:35447-35455.
- 639 51. **Mora-Montes HM, Netea MG, Ferwerda G, Lenardon MD, Brown GD, Mistry AR,**
640 **Kullberg BJ, O'Callaghan CA, Sheth CC, Odds FC, Brown AJ, Munro CA, Gow**

641 NA. 2011. Recognition and blocking of innate immunity cells by *Candida albicans* chitin.
642 Infect. Immun. **79**:1961-70.
643 52. **Jahn B, Langfelder K, Schneider U, Schindel C, Brakhage AA.** 2002. PKSP-
644 dependent reduction of phagolysosome fusion and intracellular kill of *Aspergillus*
645 *fumigatus* conidia by human monocyte-derived macrophages. Cell. Microbiol. **4**:793-803.
646
647

648

649

650 **Figures legends**

651 **Figure 1:** Melanin biosynthetic pathway – schematic representation.

652

653 **Figure 2:** Effect of melanin biosynthetic pathways mutant conidia on the maturation of human
654 dendritic cells. Immature DCs (0.5×10^6 cells/ml) were cultured in the presence of cytokines GM-
655 CSF and IL-4 (Ctr DC) or with cytokines and WT conidia or melanin biosynthetic pathways
656 mutant conidia ($\Delta pksP$, $\Delta ayg1$, $\Delta arp2$, $\Delta arp1$, $\Delta arb1$, $\Delta arb2$) at 1:1 ratio for 48 hours. The
657 percentage expression of (A) CD83, (B) CD86, and mean fluorescence intensities (MFI) of (C)
658 CD80 and (D) CD40 were analyzed by flow cytometry. Data (mean \pm SEM) are from four to five
659 donors. The level of statistical significance is indicated (* $P < 0.05$, ** $P < 0.01$).

660

661 **Figure 3:** Induction of dendritic cell cytokines by the melanin biosynthetic pathways mutant
662 conidia. Immature DCs (0.5×10^6 cells/ml) were cultured in the presence of cytokines GM-CSF
663 and IL-4 (Ctr DC) or with cytokines and WT conidia or melanin biosynthetic pathways mutant
664 conidia ($\Delta pksP$, $\Delta ayg1$, $\Delta arp2$, $\Delta arp1$, $\Delta arb1$, $\Delta arb2$) at 1:1 ratio for 48 hours. The cell-free
665 culture supernatants were analyzed for the secretion of (A) TNF- α , (B) IL-1 β , (C) IL-6 and (D)
666 IL-10. Data (mean \pm SEM) are from four donors and were presented as pg/ml. The level of
667 statistical significance is indicated (* $P < 0.05$, ** $P < 0.01$).

668

669 **Figure 4:** Effect of dihydroxynaphthalene (DHN) melanin on the phenotype, intra-cellular
670 signaling pathways and T cell stimulatory abilities of dendritic cells. (A) Immature DCs (0.5×10^6
671 cells/ml) were cultured in the presence of cytokines GM-CSF and IL-4 (negative control :Ctr-
672 DC) or with cytokines and 1 μ g of DHN melanin from WT conidia (Melanin-DC) or 1 μ g of

alkali soluble polysaccharide fraction of *A. fumigatus* cell wall (AS-DC; positive control) for 48 hours. The percentage expression of CD83, CD86, and mean fluorescence intensities (MFI) of CD80 were analyzed by flow cytometry. Data (mean \pm SEM) are from four donors. (B) DCs were treated with 1 μ g of DHN melanin from WT conidia (left panels) or 1 μ g of alkali soluble polysaccharide fraction of *A. fumigatus* cell wall (AS; positive control) (right panels) for indicated time points. The phosphorylation of ERK1/2 (pERK1/2) and p38 MAPK (pp38) was analyzed by immunoblotting. Unstimulated condition is represented by *Med.* (C) DCs were cultured in the presence of cytokines GM-CSF and IL-4 (negative control: Ctr-DC) or cytokines and 1 μ g of melanin extracts from WT conidia or cytokines and 1 μ g of alkali-soluble (AS) fraction (positive control: AS-DC) for 48 hours. Following extensive washing, DCs were co-cultured with CD4⁺ T cells at various DC:T cell ratios. The T cell proliferation was quantified by (³H) thymidine incorporation and values are presented as counts per minute (cpm). (D) The CD4⁺ T cell cytokines IL-2, IFN- γ and IL-5 in the above DC-T cell co-cultures were quantified and presented as pg/ml. Data (mean \pm SEM) are from four donors. The level of statistical significance is indicated (*P<0.05, **P<0.01).

Figure 5: AFM imaging reveals that the loss of melanin correlates with the lack of exposed rodlet layer. AFM deflection images of the surface of $\Delta pksP$ (A-C), $\Delta ayl1$ (D-F), $\Delta arp2$ (G-I), $\Delta arp1$ (J-L) and WT (M-O) conidia recorded in deionized water at low (A,D,G,J,M), medium (B,E,H,K,N) and high (C,F,I,L,O) resolutions. Black labels R and A indicate regions made of rodlets and amorphous materials, respectively.

695 **Figure 6:** SDS-PAGE (15% gel) profile of the RodAp extracted from the WT and melanin
696 biosynthetic pathway mutant conidial surfaces using hydrofluoric acid (HF). Protein bands were
697 revealed by silver staining. RodAp* represents degraded form of RodAp due to HF-treatment.

698

699 **Figure 7:** Structural modifications influence the conidial surface hydrophobicity. AFM deflection
700 images (A,D,G,J,M) recorded in deionized water, together with adhesion force maps (x-y: 1 μ m x
701 1 μ m; z-range: 3 nN) (B,E,H,K,N) and corresponding adhesion histograms (n=1024) (C,F,I,L,O)
702 recorded with hydrophobic tips on the surface of $\Delta pksP$ (A-C), $\Delta ayg1$ (D-F), $\Delta arp2$ (G-I), $\Delta arp1$
703 (J-L) and WT (M-O).

704

705 **Figure 8:** ConA-FITC labeling of $\Delta pksP$, $\Delta ayg1$ and WT strain resting conidia. Note the increase
706 in the ConA labeling on the $\Delta pksP$ mutant conidial surface compared to Wt and $\Delta ayg1$ conidia.
707 Scale bar: 10 μ m.

708

709 **Figure 9:** NaCl extracted proteins from the surface of mutant and WT resting conidia. SDS-
710 PAGE (10% gel) of proteins extracted after 2 h incubation of resting conidia in 0.5 M NaCl.

711

712 **Figure 10:** Effect of NaCl extracts from the surface of mutant and WT resting conidia on the
713 maturation of dendritic cells. Immature DCs were cultured in the presence of cytokines GM-CSF
714 and IL-4 (Ctr DC) or cytokines and NaCl-extracts from the surface of WT resting conidia or
715 mutant conidia ($\Delta pksP$, $\Delta ayg1$, $\Delta arp2$, $\Delta arp1$) for 48 hours. The percentage expression of (A)
716 CD86, and mean fluorescence intensities (MFI) of (B) CD80 and (C) CD40 were analyzed by
717 flow cytometry. Data (mean \pm SEM) are from four donors. The level of statistical significance is
718 indicated (*P<0.05, **P<0.01).

719 **Figure 11:** WGA-FITC labeling of mutant and WT resting conidia. Note the decreasing number
720 of ConA-positive conidia of the first mutants of the melanin pathway to last one. Scale bar: 10
721 μm .

722

723 **Table 1:** Identification of the proteins extracted from the $\Delta pksP$ mutant conidial surface.

724 Identification was done by MS/MS and MS with a mascot score above a threshold of 54.

Locus tag	Accession	Name
AFUA_6G12070	gi 70992475	FAD binding domain protein
AFUA_5G09580	gi 83305637	Hydrophobin RodAp
AFUA_3G02270	gi 70986104	mycelial catalase Cat1p
AFUA_8G00630	gi 70983229	conserved hypothetical protein
AFUA_1G05770	gi 70990956	exo- β -1,3-glucosidase ExoG2p
AFUA_4G09280	gi 70994100	conserved hypothetical protein
AFUA_1G03600	gi 70990522	exo- β -1,3-glucanase Exg1p
AFUA_3G15090	gi 146323525	adenosine deaminase family protein
AFUA_2G11440	gi 71001590	proteasome component Pup2p
AFUA_6G06350	gi 70991357	proteasome subunit alpha type 3
AFUA_6G04790	gi 70984160	proteasome component Pre5p
AFUA_7G04650	gi 70987129	proteasome component Pre3p
AFUA_3G11300	gi 70999540	proteasome component Prs2p
AFUA_6G06450	gi 70991377	proteasome component Pre4p
AFUB_042910	gi 159128006	cytoskeleton assembly control protein Sla2p, putative
AFUA_7G06140	gi 70986816	Putative secreted 1,4- β - D-glucan glucanhydrolase
AFUA_1G12610	gi 70995752	Hsp70 chaperone Hsp88p
AFUA_8G05020	gi 70983560	β -N-acetylhexosaminidase NagAp
AFUA_1G14560	gi 70996140	mannosidase MsdSp

AFUA_5G12780	gi 70997246	Kelch repeat protein
AFUA_2G10660	gi 71001436	mannitol-1-phosphate dehydrogenase
AFUA_6G06440	gi 70991375	proteasome component Prs3p
AFUA_5G02330	gi 70985206	major allergen and cytotoxin AspF1
AFUA_1G13670	gi 70995964	conserved hypothetical protein
AFUA_3G13465	gi 146323476	conserved hypothetical protein
AFUA_2G11900	gi 71001682	pyruvate dehydrogenase kinase
AFUA_4G03490	gi 70982015	tripeptidyl-peptidase (TppAp)
AFUA_1G04130	gi 70985206	FG-GAP repeat protein
AFUA_3G00590	gi 70985747	Asp-hemolysin
AFUB_018320	gi 159128674	β -fructofuranosidase, putative
AFUA_1G12170	gi 70995660	translation elongation factor EF-Tu
AFUA_5G00700	gi 70985526	hypothetical protein AFUA_5G00700
AFUA_8G01980	gi 70982961	conserved hypothetical protein
AFUA_1G13670	gi 70995964	conserved hypothetical protein
AFUA_2G06150	gi 70989789	protein disulfide isomerase Pdi1p
AFUA_6G04570	gi 70984206	translation elongation factor eEF-1 subunit gamma
AFLA_093140	gi 238499799	histone H3 methyltransferase, putative
AFUA_3G07810	gi 71000275	succinate dehydrogenase subunit Sdh1p
AFUA_8G01410	gi 70983075	class V chitinase ChiB1p
AFUA_3G11690	gi 70999466	fructose-bisphosphate aldolase, class II
AFUB_007340	gi 159130919	pyruvate dehydrogenase E1 component α -subunit, putative

Figure 1

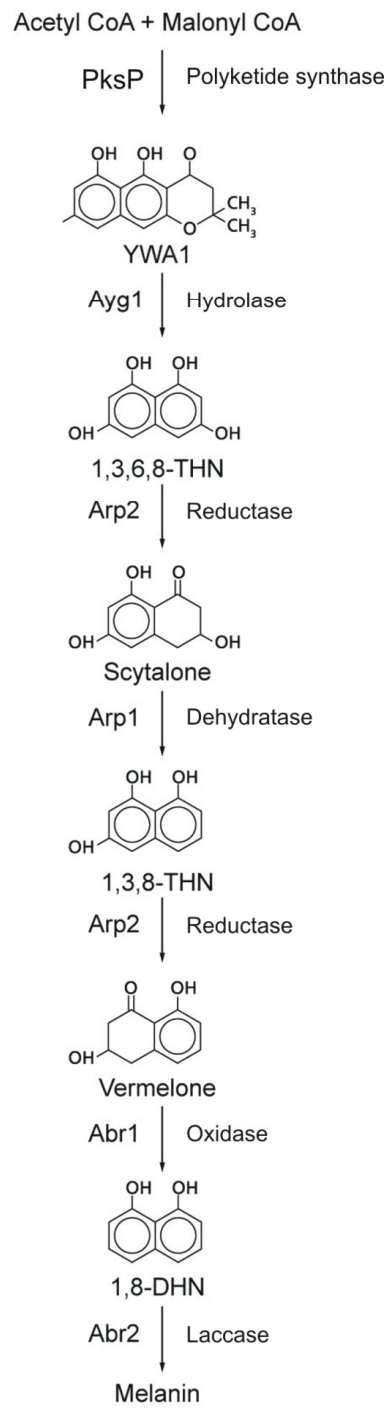


Figure 2

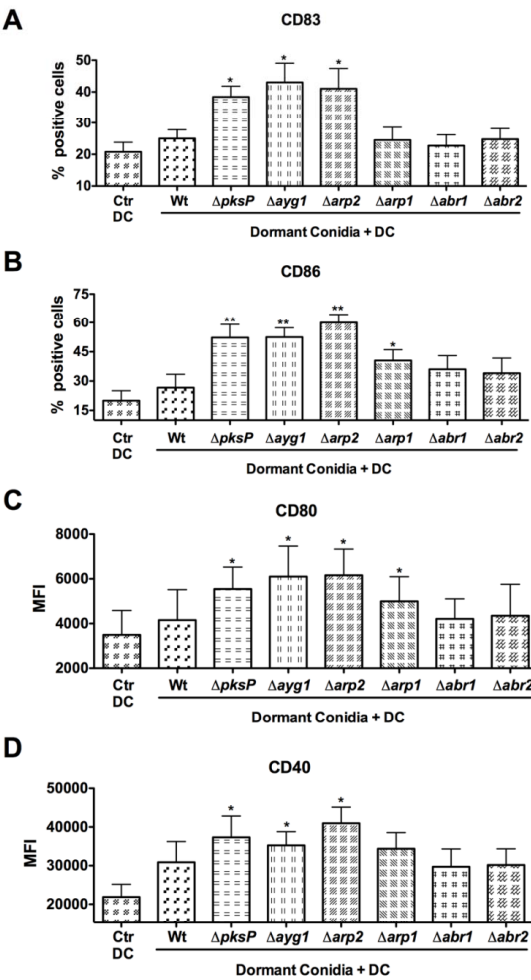


Figure 3

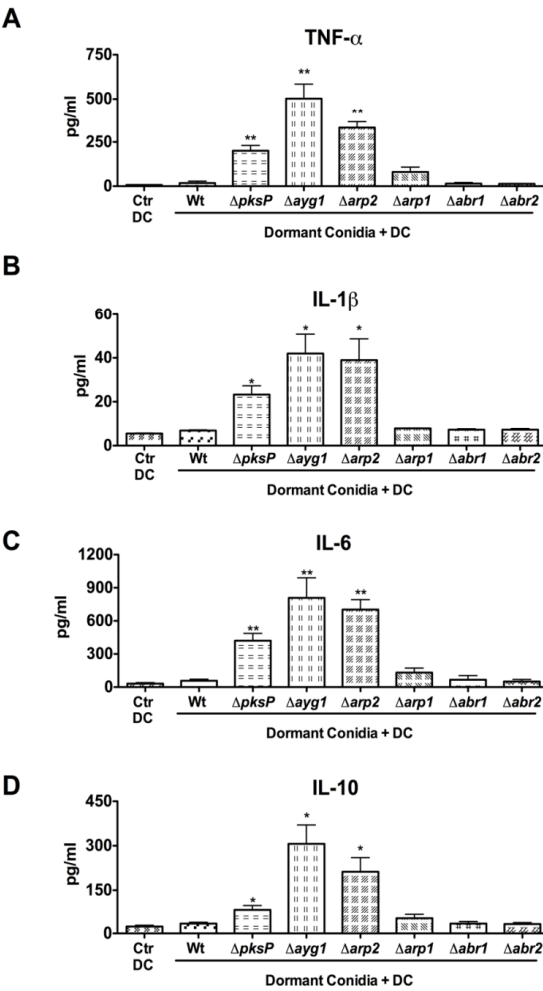


Figure 4

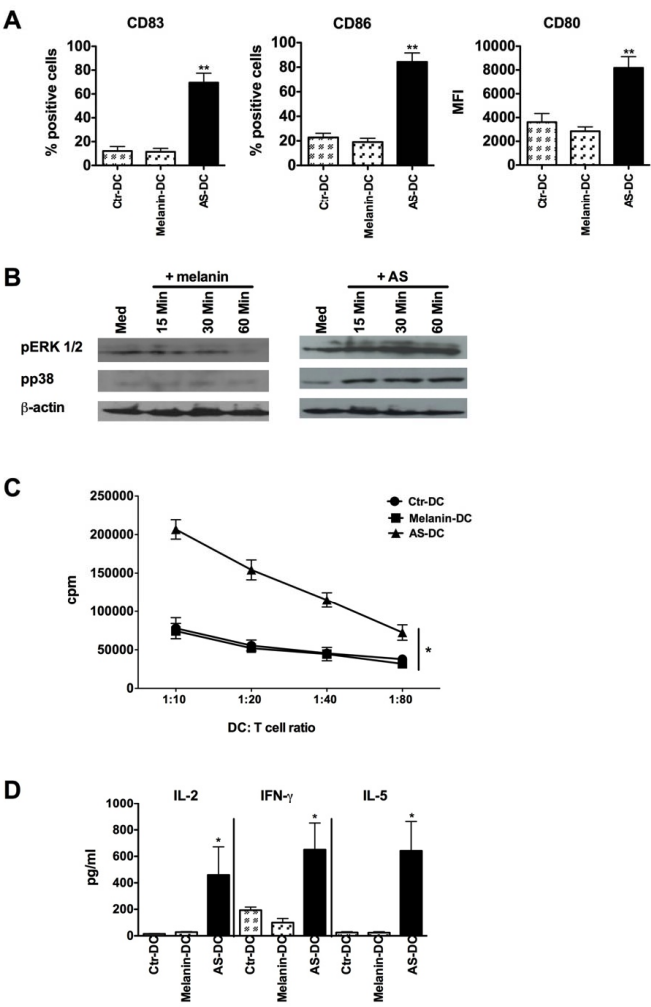


Figure 5

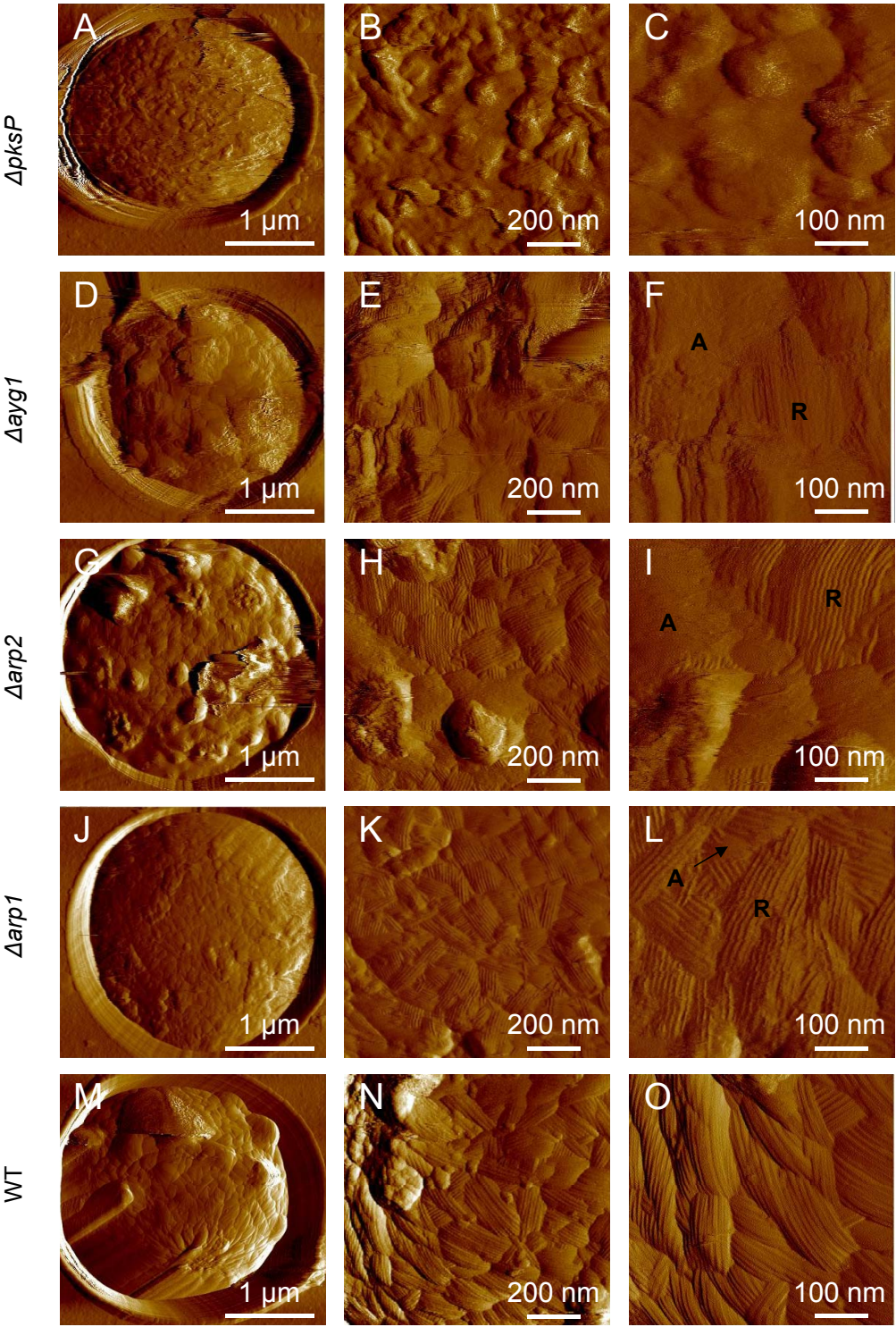


Figure 6

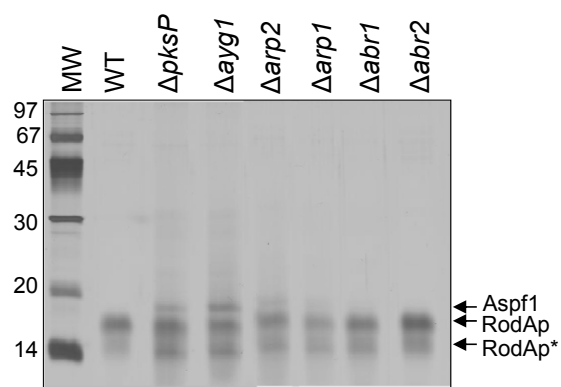


Figure 7

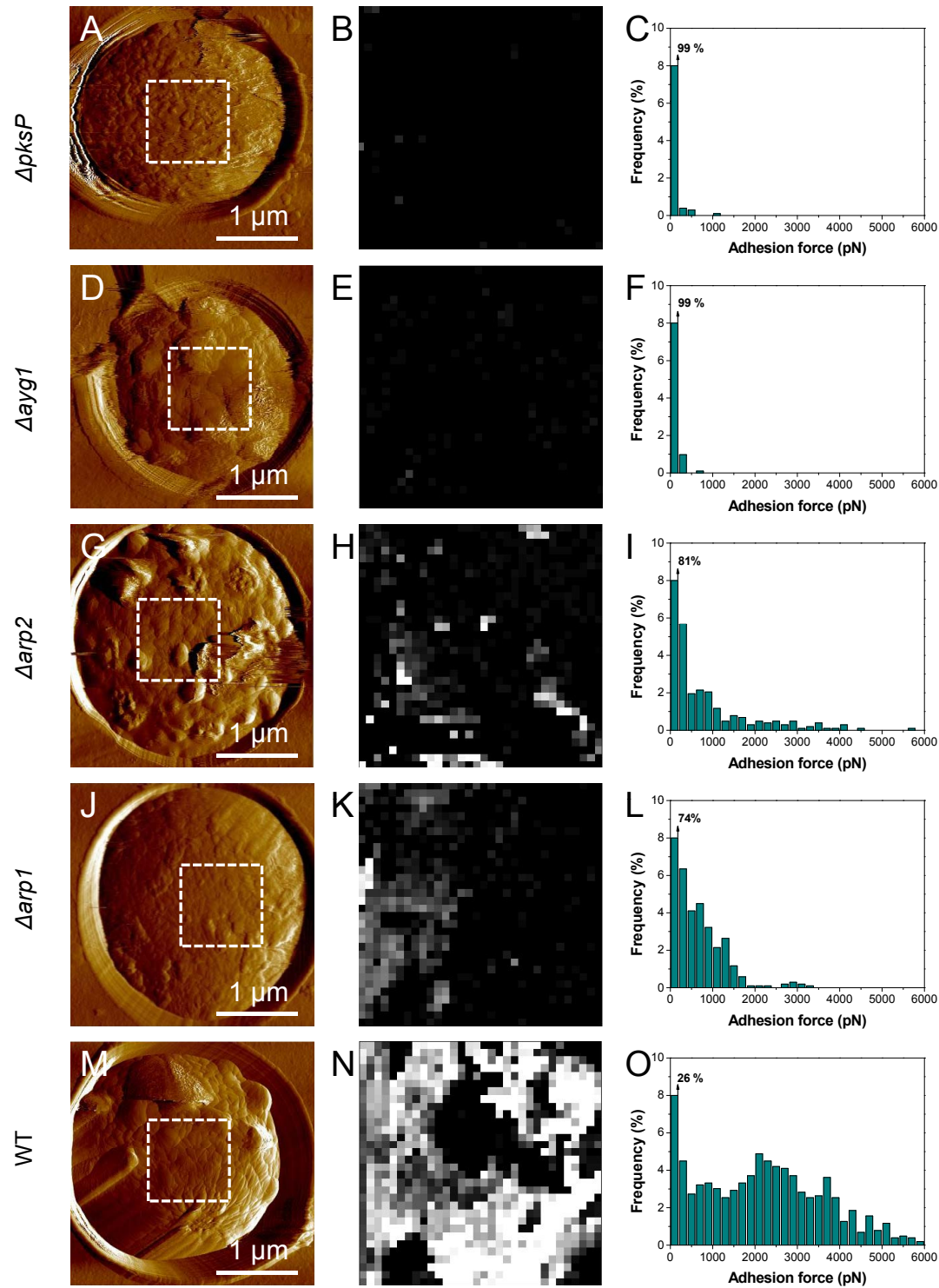


Figure 8

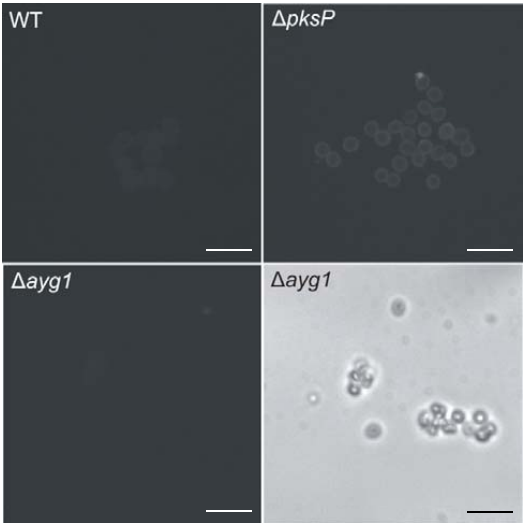


Figure 9

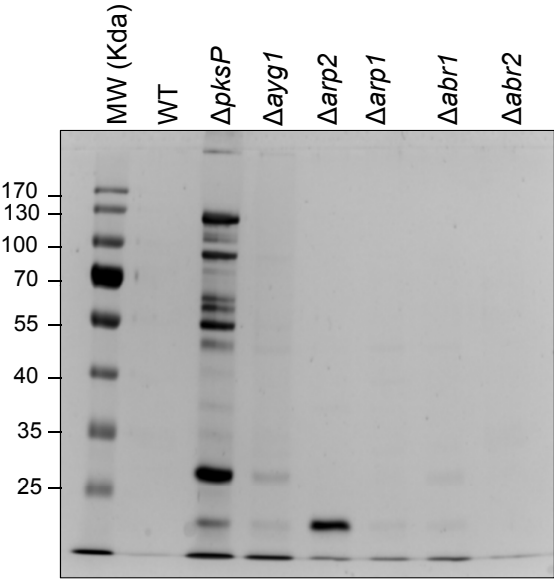


Figure 10

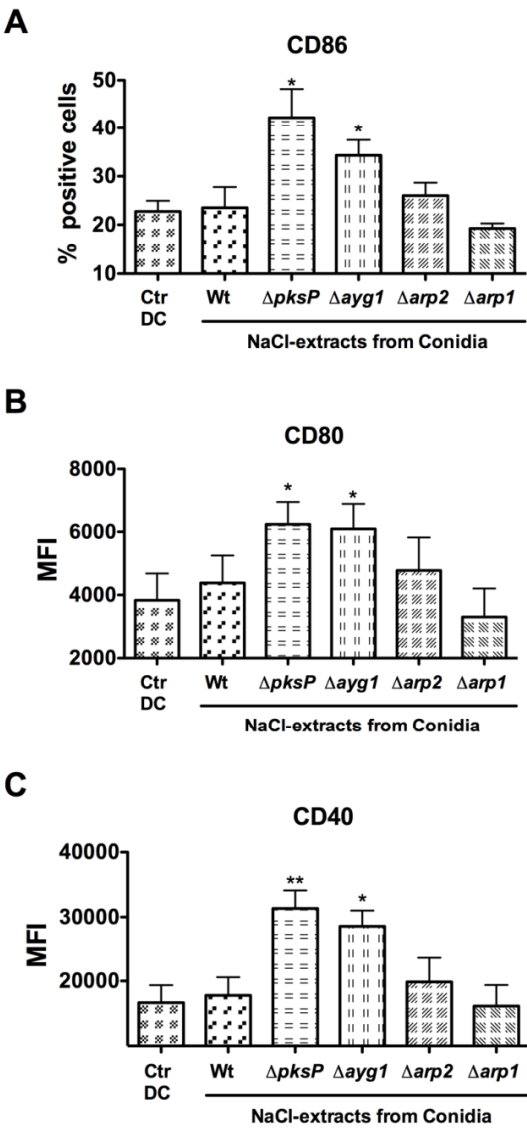


Figure 11

